Dielectrophoretic trapping of selenium nanorods for use in device applications

Seyed Reza Mahmoodi · Marzieh Bayati ·
Somayeh Hosseini Rad · Elham Kamali Heidari ·
Alireza Foroumadi · Kambiz Gilani

Abstract Dielectrophoretic alignment of the Selenium (Se) nanorods is reported for electrical characterization and possible applications as micro/nano devices. Selenium nanorods were successfully synthesized using a reverse microemulsion process. The produced material was investigated structurally using X-ray diffraction and transmission electron microscope. Suspensions of the Se powder in the concentration of 0.1 (g/l) were prepared in pure ethanol. Interdigitated platinum electrodes were employed for manipulation of suspended materials in the fluid. When Se particles were exposed to the platinum electrodes in two frequencies of 10 and 100 kHz, dielectrophoretic force captured suspended particles onto the interdigitated micro-electrode array. The trapped Se nanorods were aligned along the electric field lines and bridged the electrode gaps. Dielectrophoretic entrapment of Se nanorods on microelectrode was also detected by impedance measurements. The device was characterized and can potentially be used as a nanodevice.

S. R. Mahmoodi · M. Bayati (✉) · S. H. Rad · E. K. Heidari
School of Advanced Technologies in Medicine, Tehran
University of Medical Sciences, No. 88, Italy Street, Qods Street,
Keshawarz Boulevard, 1417755469 Tehran, Iran
e-mail: m-bayati@tums.ac.ir

A. Foroumadi
Department of Medicinal Chemistry, Faculty of Pharmacy and
Pharmaceutical Sciences Research Center, Tehran University of
Medical Sciences, Tehran, Iran

K. Gilani
Department of Pharmaceutics, School of Pharmacy, Tehran
University of Medical Sciences, Tehran, Iran

1 Introduction

One-dimensional nanostructures have distinctive properties in mechanical, chemical and electronic aspects. They have recently attracted considerable research interest due to their novel properties and their potential applications in device miniaturization [1]. Precise and reliable handling of these nanomaterials is necessary for the characterization of their electrical and mechanical behavior, the analysis of their response to outside agents and stimuli, and, more importantly, their eventual assembly into micro/nanodevices [2]. To this purpose, enormous efforts employing a variety of approaches have been made and reported [3, 4]. Electrokinetic manipulation has been recognized as a useful technique for separation, alignment and positioning of microscopic objects, owing to its simple implementation and reliability from no moving parts [5]. Two types of electrokinetics are worth to consider, DC and AC. Although using DC electric fields is important for manipulation of nanoscale materials, high voltage operation and consequently excessive electrochemical reactions and electrolysis at electrodes make it less attractive in nanomaterials manipulation. Low operating voltage, minimizing electrolysis and chemical reactions, along with nonlinear nature of AC electrokinetics prove to be more suitable for the operation of particles on micro/nano scales [6].

Dielectrophoresis (DEP) arises from interaction of a non-uniform electric field with the induced dipoles in the particles and is one of the most commonly used techniques for characterization, separation, orientation and precise manipulation of micrometer and sub-micrometer particles suspended in fluid media [5–7]. Particles will be attracted towards high/low electric field regions depending on the relative polarizability of the particle and the medium.

One-dimensional nanostructures are ideal DEP target materials due to their high aspect ratios [6, 7].

Selenium is an important elemental semiconductor due to its high photoconductivity, large piezoelectric, and thermoelectric effects. Owing to its unique properties, Se has been extensively used in solar cells, pressure sensors, catalysts, photographic exposure meters, xerography, electrical rectifier, etc. [8, 9]. Se is also one of the essential elements for human well being. It has been confirmed that Se can improve the activity of the seleno-enzyme, gluta-thione peroxidase and prevent free radicals from damaging cells and tissues in vivo [10, 11]. Recently, much effort has been devoted to the fabrication of selenium nanostructures due to their excellent photoelectric performance and high biological activity [11]. Different synthetic approaches have been used for synthesis of Se nanostructures such as pulse laser ablation [12], chemical vapor deposition [13] or wet chemical methods such as templating route [14] and sonochemichal process [15]. Among all these techniques, the microemulsion process proves to be a promising method for synthesizing ultrafine inorganic powders [16, 17]. The main advantage of using microemulsions to synthesize selenium nanostructures is in fact that by simple adjustment of the molar ratio of water with respect to surfactant, the precision control of particles shape and corresponding size distributions may be achieved [18].

Most of the works on AC electrokinetics have been focused on biological particles, gold and carbon nanotubes so far [19] and only limited research is devoted to the interaction between AC electrokinetics and Se nanostructures. Liu et al. [9] used DEP for extracting an individual tube from solution by the tungsten tip of a high precision machine to perform electrical transport measurements on a single nanotube. In another study, assembly of Se nanowires into macroscopic fibers of tunable dimensions has been achieved through high voltage DC electric field [20]. In our previous research, assembly of the Se nanoparticles through different AC electrokinetic phenomena on microelectrode arrays has been reported [21]. In this manuscript, reverse microemulsion process has been applied for synthesis of Se nanorods. AC electric field was used to manipulate the Se nanorods between microelectrodes for electrical characterization and investigating potential application as a nano-photo-sensor. It was shown that impedance measurement techniques have the potential for detection of non-biological particles in non-aqueous solutions.

2 Materials and methods

T-Se nanorods were prepared by reverse-microemulsion process at room temperature. First, in a cyclic method the precursor for Se that is, sodium seleno sulfite (Na_2SeSO_3) solution was prepared by dissolution of Se powder (Merck, Germany) in hot (80 °C) sodium sulfite (Merck, Germany) [22]. The synthesized Na_2SeSO_3, 2.0 mol/l HCl solution and analytical grade of cyclohexane (Merck, Germany), sodium dodecane (SDS) (Sigma Aldrich Inc., USA) and n-butanol (Merck, Germany) were used as starting materials. After that, the preparation process of microemulsion solutions was performed based on the method described in detail elsewhere [23]. The product powder, suspended in the two phases interface, was separated by centrifuge, and washed with acetone, deionized water and ethanol for several times, and then dried in a vacuum at room temperature. Powder X-ray diffraction (XRD, Philips PW1710 with Cu Kα radiation) and TEM equipped with an Energy Dispersive X-Ray Spectroscopy (EDX) were employed for characterization of the as-prepared products.

Interdigitated microelectrodes were fabricated from Platinum on a glass surface (Delta Technologies Ltd., Stillwater, MN, USA). The distance between adjacent electrodes was 30 μm and the electrode strips had nearly the same widths. A DEP chamber was constructed on top of the microelectrodes from glass slides and epoxy sealant. The chamber had a length of 35 mm, a width of 25 mm, and a height of 600 μm. A digital Camera (CMEX DC.1301, Euromex was mounted on a biological microscope (FE 2025, Euromex) for continuous monitoring the chamber and photographic recording of particles patterning. Suspensions of the synthesized powder in the concentration of 0.1 (g/l) were prepared in absolute ethanol (Merck, Germany) by sonication for 5 min and subsequently flushed into the DEP chamber through a syringe. Microelectrode devices were energized using a function generator (RIGOL DG 1022). AC signal was applied with the amplitude of 10 V_{p-p} (peak to peak voltage) at two frequencies of 10 and 100 kHz with sinusoidal waveform. In order to electrically characterize the fabricated device, the DEP process was continued until the solution was completely dried out at room temperature. Since the formation of Se nanorod bridges between the electrodes mostly happened at the frequency of 10 kHz, only the DEP-processed sample at this frequency was employed for electrical characterizations.

Electrochemical impedance spectroscopy (EIS) analyses were performed by applying an AC oscillation of 0.1 V_{p-p} in the frequency range of 0.01 Hz to 1 MHz. The current–voltage (I–V) measurements were performed on DEP-patterned microelectrode using an Autolab PGSTAT 30 analyzer. Aligned Se nanorods in DEP chamber were illuminated by a 25 W Tungsten filament lamp in a light and noise shield box, and the electrode current with a bias voltage of 1 V was measured with an input time constant of 1 s.

3 Results and discussion

Se nanorods were synthesized by the reaction of Na_2SeSO_3 under acidic conditions in micellar solutions of the SDS anionic surfactant. Figure 1a presents a low-magnification TEM image of the microemulsion-derived product, which suggests that the product shows exclusive rodlike morphology with lengths ranging from several micrometers to more than 20 μm. High-magnification TEM images of the product powder (Fig. 1b) revealed that the nanorods' diameters scale from tens of nanometers to more than 100 nm. The XRD spectrum of the synthesized powder is shown in Fig. 2a indicating that the product is fully crystalline with trigonal crystal structure. The corresponding spectrum of EDX analysis (Fig. 2b) also confirms the pure composition of Se nanorods.

An AC electrical field was applied to the microelectrodes after the medium was syringed into the chamber. The frequencies in the approximate range of 1–100 kHz were observed to be the effective frequencies to capture the nanorods from the solution by positive DEP. At both
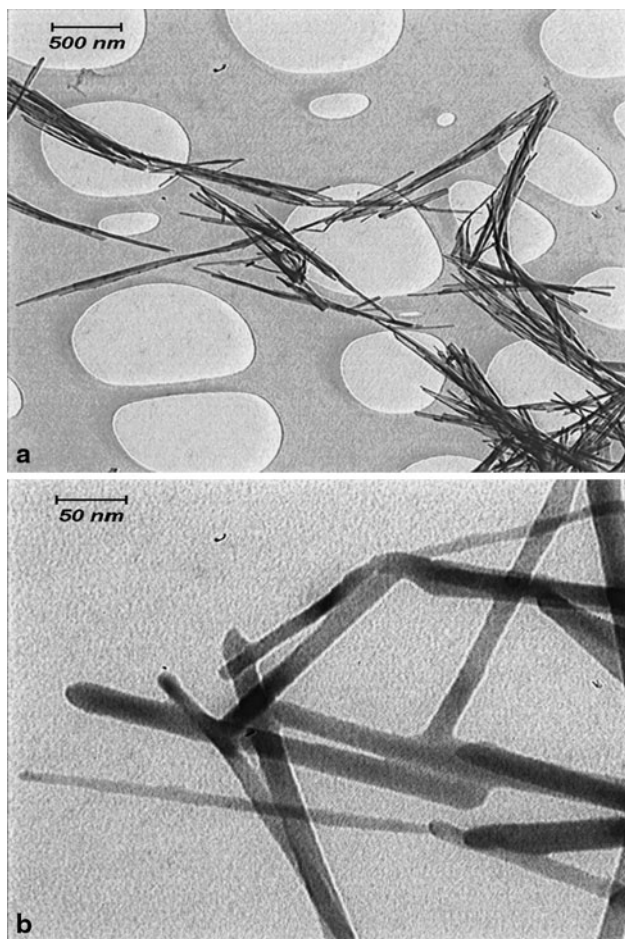

Fig. 1 a Low and b high-magnification TEM images of Se nanorods grown by a reverse microemulsion method
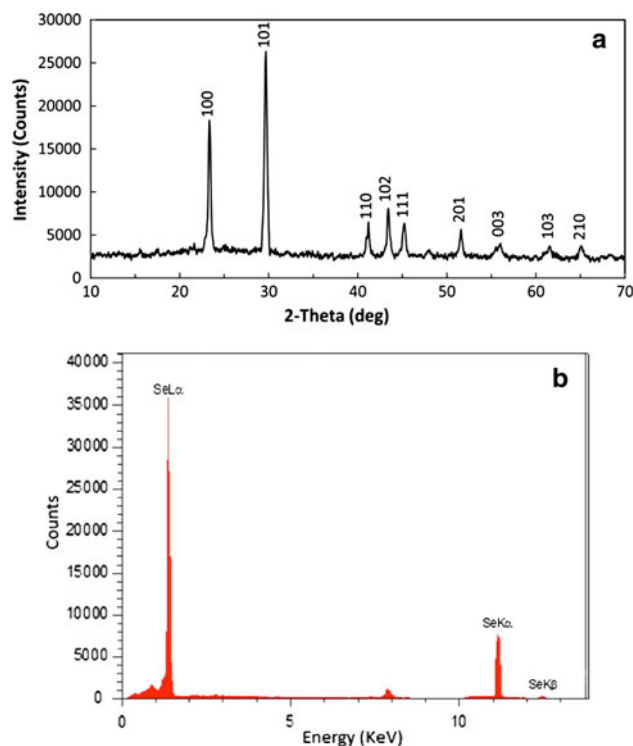

Fig. 2 a XRD pattern and b EDX spectrum of reverse-microemulsion derived Se nanorods

applied frequencies (10 and 100 kHz), the Se nanorods were aligned across the electric field lines in a direction perpendicular to the electrode strips (Fig. 3a, b). As it can be seen from the image in Fig. 3a, Se nanorods bridged the electrode gaps linking together end to end. Also, a higher deposition yield of nanorods was observed at the frequency of 10 kHz. However, when using 100 kHz frequency, no or very few bridges formed between the electrode pairs across the whole electrode. A higher magnification image of the electrode gap in Fig. 3c depicts that the solution of particles contains a mixture of nanorods and debris particles, which could have been produced during dispersion (sonication). Moreover, the image shows more clearly how Se nanorods and debris particles attach together to create connection between the two neighboring electrode strips.

There are methods other than photographic recording through a microscope, which have been developed to probe the DEP collection of particles on electrodes [24]. One of these methods is based on measuring changes of the electrode impedance. Several studies [25–27] have combined DEP and EIS methods to detect biological particles on interdigitated electrodes arrays. To investigate this issue, the impedance spectrum of the microelectrode was measured before and after the DEP manipulation at 10 and 100 kHz frequencies (Fig. 4). Comparing with the "before DEP" spectrum, a drop in the measured impedance after DEP manipulation at 10 kHz is observable in the 100 Hz–1 MHz
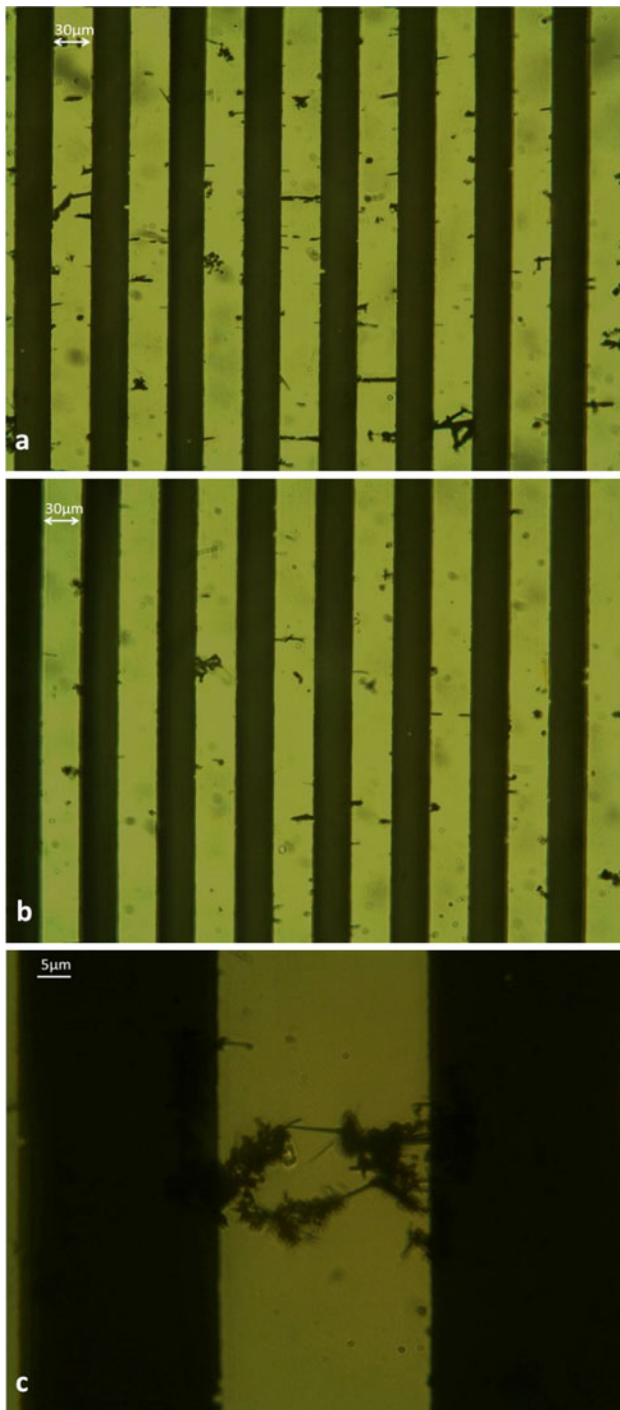
Fig. 3 Microscope images of particles trapped onto the microelectrode by DEP at two frequencies of **a** 10 kHz-Lower magnification, **b** 100 kHz-Lower magnification and **c** 10 kHz- Higher magnification

Fig. 4 Impedance spectrum of the microelectrode before and after the DEP manipulation of the Se nanoparticles

Fig. 5 Temporal variation of the electrode impedance, measured during the DEP process at the two frequencies of 10 and 100 kHz

frequency range. The drop in the impedance for 100 kHz DEP sample is smaller and is limited to the 1–100 kHz frequency range. It is noteworthy that the measured impedance responses demonstrate very good repeatability.

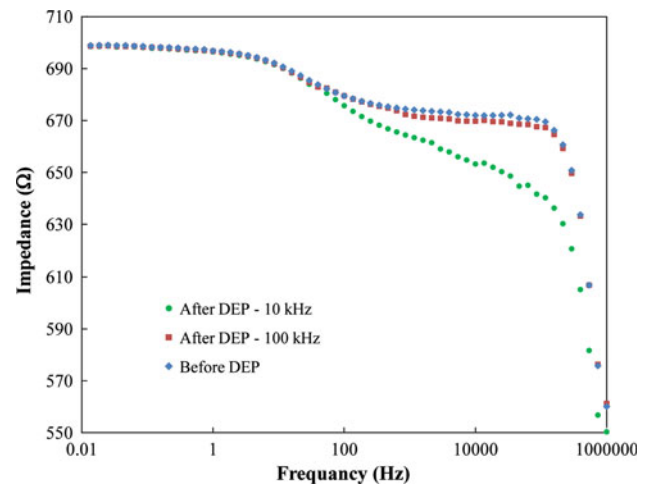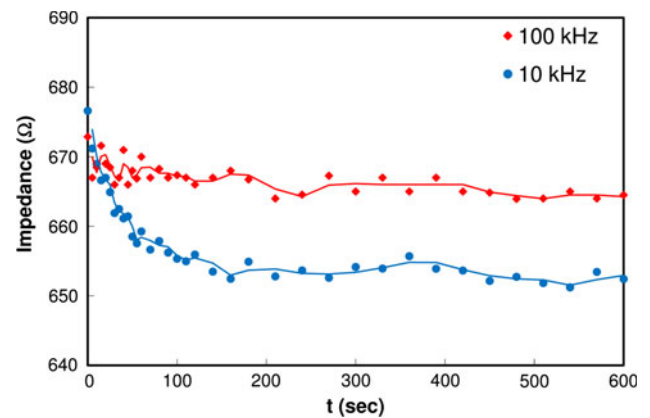Zou et al. [28] have studied the impedance changes phenomena in aqueous solutions by EIS sensing. They have attributed these alterations in impedance spectra to the deposition patterns of particles. Our achieved results are in good agreement with their findings and accordingly the impedance reduction in our work has possibly happened due to the variation in the average conductivity of the medium that separates the opposite electrodes [29]. The variation of impedance during the DEP process for the two applied frequencies is demonstrated in Fig. 5. In the 10 kHz condition, the impedance is seen to decrease with decreasing rate and it reaches a plateau nearly after 200 s after applying the AC signal, whereas the 100 kHz curve doesn't show a significant change of the impedance during the DEP process.

It has previously been reported [30] that the technique of impedance monitoring during DEP process (dielectrophoretic impedance measurement, DEPIM) has the potential to control the assembly of particles between the sensor electrodes. This feature provides the possibility to define the normalized sensitivity of the fabricated sensor. However,
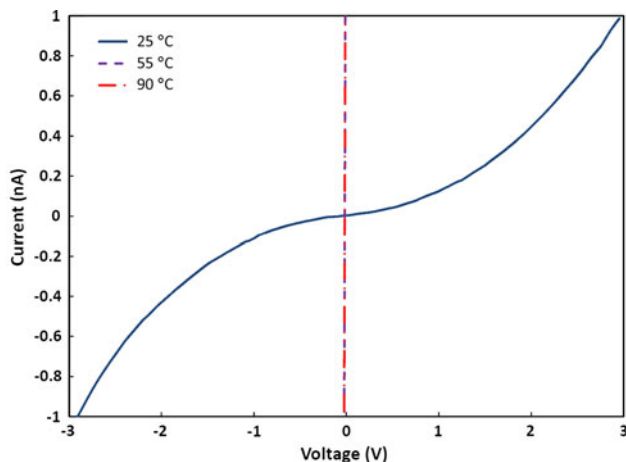
Fig. 6 I–V (current–voltage) characteristics of the DEP-trapped Se nanorods on microelectrode at three temperatures of 25, 55 and 90 °C
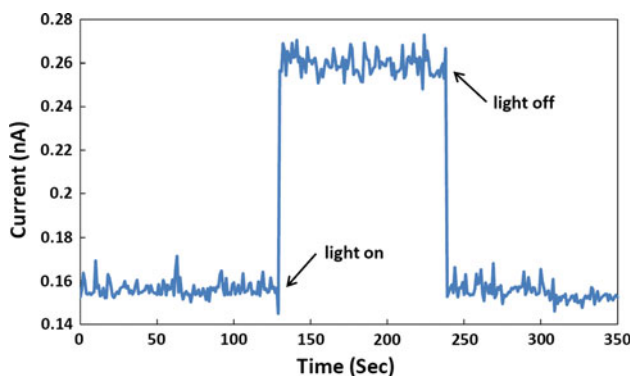

Fig. 7 Transient photoresponse of DEP-aligned Se nanorods at a bias of 1 V

a *p*-type extrinsic semiconductor occurs due to valence band hole transport [31]. Although the measured light sensitivity is not much significant, such short response time is essential for the design and development of optical sensors. The possible reason for rather low sensitivity may be explained by large electrode spacings of the light sensor in compare with the average length of the nanorods. Although, linking of particles together to make connections between the electrodes may lead to limitations in some sensitivity cases, this phenomenon is promising to investigate the characteristics of orderly assembled nanostructured materials. For this purpose, DEP provides a rapid and simple method which otherwise would be costly if employing techniques based on high precision machines.

4 Conclusion

A Se nanorod-based UV photosensor was successfully fabricated by applying positive DEP on a microelectrode array. The Se nanorods were synthesized by a reverse micro-emulsion method. The DEP-trapping of the Se nanorods between the electrode gaps was investigated by DEPIM and EIS methods. Aligned nanorods on the microelectrode were electrically examined and then illuminated by a tungsten light source, which led to an increase in conductance followed by a rapid saturation. Compared to machine based methods, DEP can provide a more convenient method for constructing micro/nanoscale photodetectors.

our achieved data can demonstrate that DEPIM technique done in a specific frequency may not be applicable to control the DEP assembly in all ranges of the applied DEP frequency, especially when the entrapment yield of particles is small. On the contrary, EIS measurements enable to detect particles through monitoring the conductivity and/or capacitance changes at electrode surface in the DEP and/or other frequencies and, therefore, can provide a better understanding of the situation.

I–V measurements of the DEP-aligned sample were conducted at three temperatures of 25, 55 and 90 °C (Fig. 6). As it can be seen from Fig. 6, the I–V characteristic at 25 °C showed a rectifying behavior. At higher temperatures linear behaviors with slopes of $2 \times 10^{-6} \, \Omega^{-1}$ (55 °C) and $5 \times 10^{-6} \, \Omega^{-1}$ (90 °C) were observed. For the light sensitivity test, as illustrated in Fig. 7, the conductance of the DEP assembled electrode was increased and saturated rapidly when the Se nanorods exposed to illumination of light source, and it decreased back to the initial value when the light was turned off. Conduction in t-Se as

References

1. S.V.N.T. Kuchibhatla, S. Karakoti, D. Bera, S. Seal, One dimensional nanostructured materials. Prog. Mater. Sci. **52**(5), 699–913 (2007)
2. S. Evoy, M. Riegelman, N. Naguib, H. Ye, P. Jaroenapibal, D.E. Luzzi, Y. Gogotsi, dielectrophoretic assembly of carbon nanofiber nanoelectromechanical devices. IEEE transactions on nanotechnology, **4**(5) (2005), 570–575
3. F. Patolsky, C.M. Lieber, Nanowire nanosensors. Mater. Today **8**(4), 20–28 (2005)
4. L. Dai, A. Patil, X. Gong, Z. Guo, L. Liu, Y. Liu, D. Zhu, Aligned Nanotubes. Chem. Phys. Chem. **4**, 1150–1169 (2003)
5. H. Morgan, N.G. Green, AC Electrokinetic: Colloids and Nanoparticles, Research Studies Press Ltd. Baldock, Hertfordshire, England., 2002
6. M. P. Hughes, Nanoelectromechanics in engineering and biology, CRC PRESS, 2–15, Boca Raton, florida, USA, 2003
7. M.P. Hughes, AC electrokinetics: applications for nanotechnology. Nanotechnology **11**(2), 124 (2000)
8. L. Qi, W. Shen, Selective synthesis of single-crystalline selenium nanobelts and nanowires in micellar, solutions of nonionic surfactants (14) (2005), 6161–6164

9. P. Liu, Y. Ma, W. Cai, Z. Wang, J. Wang, L. Qi, D. Chen, Photoconductivity of single-crystalline selenium nanotubes. Nanotechnology **18**, 205704 (2007)

10. B. X. Gao, J. Zhang, L. Zhang, Hollow sphere selenium nanoparticles: Their In-vitro anti hydroxyl radical effect, Advanced Materials (**4**) (2002), 2000–2003

11. S. Zhang, J. Zhang, H. Wang, H. Chen, Synthesis of selenium nanoparticles in the presence of polysaccharides. Mater. Lett. **58**, 2590–2594 (2004)

12. M. Quintana, E. Haro-poniatowski, J. Morales, N. Batina, Synthesis of selenium nanoparticles by pulsed laser ablation. Appl. Surf. Sci. **195**(1–4), 195 (2002)

13. X. Cao, Y. Xie, L. Li, Spontaneous organization of three-dimensionally packed trigonal selenium microspheres into large-area nanowire networks. Adv. Mater. **15**, 1914–1918 (2003)

14. Q. Lu, F. Gao, S. Komarneni, Cellulose-directed growth of selenium nanobelts in solution **30**, 159–163 (2006)

15. B.T. Mayers, K. Liu, D. Sunderland, Y. Xia, Sonochemical synthesis of trigonal selenium nanowires. Chem. Mater. **15**(20), 3852–3858 (2003)

16. S.K. Haram, A.R. Mahadeshwar, S.G. Dixit, Synthesis and characterization of copper sulfide nanoparticles in triton-x 100 water-in-oil microemulsions. J. Phys. Chem **100**(14), 5868–5873 (1996)

17. C.C. Chang, J.Y. Kim, P.N. Kumta, Synthesis and electrochemical characterization of divalent cation-incorporated lithium nickel oxide. J. Electrochem. Soc. **147**(5), 1722–1729 (2000)

18. C. Lu, H. Wang, Reverse-microemulsion preparation and characterization of ultrafine orthorhombic LiMnO 2 powders for lithium-ion secondary batteries. J. Eur. Ceram. Soc. **24**, 717–723 (2004)

19. Y.K. Seo, S. Kumar, G.H. Kim, Dielectrophoretic alignment of ZnO nanoparticles in pre-patterned nanogap electrodes, 9th IEEE Conference on Nanotechnology (2009) 264–266

20. S. Wang, M.C.P. Zhang, X. Majidi, E. Nedelec, K. Gates, B.D. Nantes et al., Electrokinetic assembly of selenium and silver nanowires into macroscopic fibers. ACS Nano **4**(5), 2607–2614 (2010)

21. S.R. Mahmoodi, M. Bayati, S. Hosseinirad, A. Foroumadi, K. Gilani, S.M. Rezayat, AC electrokinetic manipulation of selenium nanoparticles for potential nanosensor applications. Mater. Res. Bull. **48**(3), 1262–1267 (2013)

22. J.E. Hoffmann, M.G. King, *Selenium and Selenium Compounds* (John Wiley and Sons, Inc., Kirk-Othmer Encyclopedia of Chemical Technology, 2001)

23. M.Z. Liu, S.Y. Zhang, Y.H. Shen, M.L. Zhang, Selenium nanoparticles prepared from reverse microemulsion process. Chin. Chem. Lett. **15**(10), 1249 (2004)

24. R. Pethig, Review article-dielectrophoresis: status of the theory, technology, and applications. Biomicrofluidics **4**(2), 1–35 (2010)

25. S.K. Mohanty, S.K. Ravula, K.L. Engisch, A.B. Frazier, in *A micro system using dielectrophoresis and electrical impedance spectroscopy for cell manipulation and analysis*. 12th International Conference on Transducers, Solid-state Sensors, Actuators and Microsystems, vol. 2 (2003), pp. 1055–1058

26. L. Yang, Electrical impedance spectroscopy for detection of bacterial cells in suspensions using interdigitated microelectrodes. Talanta **74**(5), 1621–1629 (2008)

27. M. Varshney, Y. Li, Interdigitated array microelectrodes based impedance biosensors for detection of bacterial cells. Biosens. Bioelectron. **24**(10), 2951–2960 (2009)

28. Z. Zou, S. Member, S. Lee, C.H. Ahn, A polymer microfluidic chip with interdigitated electrodes arrays for simultaneous dielectrophoretic manipulation and impedimetric detection of microparticles. Sens. J. IEEE **8**(5), 527–535 (2008)

29. D.W.E. Allsopp, L.R. Milner, A.P. Brown, W.B. Betts, Impedance technique for measuring dielectrophoretic collection of microbiological particles. J. Phys. D Appl. Phys. **32**, 1066–1074 (1999)

30. J. Suehiro, R. Yatsunami, R. Hamada, M. Hara, Quantitative estimation of biological cell concentration suspended in aqueous medium by using dielectrophoretic impedance measurement method. J. Phys. D Appl. Phys. **32**(21), 2814–2820 (1999)

31. A. Qin, Z. Li, R. Yang, Y. Gu, Y. Liu, Z. Lin, Rapid photoresponse of single-crystalline selenium nanobelts. Solid State Commun. **148**, 145–147 (2008)